A REVIEW OF SOME EXSISTING DRAG MODELS DESCRIBING THE INTERACTION BETWEEN PHASES IN A BUBBLING FLUIDIZED BED

Joachim Lundberg[1], **Britt M. Halvorsen**[1,2]
1. Telemark University College
Telemark, Norway
2. Telemark Technological R&D Centre (Tel-Tek)
Telemark, Norway

joachim.lundberg@hit.no (Joachim Lundberg)

Abstract

This work represents a computational study of flow behaviour in a bubbling fluidized bed. The simulations are performed by using the commercial computational fluid dynamic (CFD) code, Fluent 6.3. The advantage of using a commercial CFD code is that corresponding cases for industrial applications can be simulated by using the same model without having very deep knowledge about the source code and the solving algorithms. In CFD simulations of fluidized beds, it is important to describe the interaction between the particles and the momentum transfer between the phases. Different models are developed for this purpose. The kinetic theory of granular flow describes the interaction between particles and is based on the kinetic gas theory. In a bubbling fluidized bed there are regions with rather low fraction of particles and regions with high particle concentrations. The bed can be described by two flow regimes, the viscous regime and the frictional regime. In the viscous regime the kinetic and the collisional stresses are dominating. The frictional regime occurs at high particle concentrations and in this regime the flow behaviour is described by friction and rubbing between the particles.

The interaction between the particles and the continuous gas phase are described by a drag model, and several drag models are developed for this purpose. The models describe the momentum exchange between the phases. The aim of this work is to study how the different drag models influence on the flow behaviour in a bubbling fluidized bed. Five different drag models have been studied. The drag models are the Gidaspow drag model, a drag model developed by Syamlal O'Brien, a customized iterative version of the drag model by Syamlal O'Brien, the modified Hill Koch Ladd drag model and the newly developed RUC drag model. Two of the drag models are included in Fluent 6.3, the other models are implemented by the author. The results from the simulations with the different drag models are compared, and the discrepancies are discussed.

1 Introduction

Fluidized beds are widely used in industrial operations, and several applications can be found in chemical, petroleum, pharmaceutical, biochemical and power generation industries. In a fluidized bed gas is passing upwards through a bed of particles supported on a distributor. Fluidized beds are applied in industry due to their large contact area between phases, which enhances chemical reactions, heat transfer and mass transfer. The efficiency of fluidized beds is highly dependent of flow behavior and knowledge about flow behavior is essentially for scaling, design and optimization.

Gravity and drag are the most dominating terms in the momentum equation of the granular phase. The application of different drag models significantly impacted the flow of the granular phase by influencing the predicted bed expansion and the particle concentration in the dense phase regions of the bed.

This paper will focus on the prediction of drag force in a fluidized bed. By other researchers several drag models are developed. In this review some of this are further investigated and compared.

To describe the properties of the particles or granular phase, models with origin in the kinetic theory for granular flow by Lun et al. [1] is chosen.

This paper is based on the master thesis by the author [2].

2 Theory of Modeling Granular flow

Modeling of granular flow is a fairly large subject and the focus has been on the models included in the commercial software Fluent 6.3. Fluent uses the Navier Stokes equations to solve a Finite volume model. The Navier Stokes equations are conservation equations of mass, momentum and energy. The energy equation has not been studied or used because compressible flow or heat transfer is not included.

The most relevant multiphase model for simulations of bubbling fluidized bed in Fluent 6.3 is the Eulerian multiphase model. This model will calculate one transport equation for momentum and one for continuity per phase. The theory for this model is taken from the reference [3].

The volume fraction for each phase is calculated with an continuity equation. Equation (1) is a example of the gas phase volume fraction equation.

$$\frac{1}{\rho_{rg}}\left(\frac{\partial}{\partial t}\left(\alpha_g\rho_g\right)+\nabla\cdot\left(\alpha_g\rho_g\,\overrightarrow{u}_g\right)=\sum_{s=1}^{n}\left(\dot{m}_{sg}-\dot{m}_{gs}\right)\right) \tag{1}$$

Index s is the granular phases and g is the gas or fluid phase. α is the volume fraction, ρ is the density, $\overrightarrow{u}$ is the phase velocity and $\dot{m}$ is the mass transfer from one phase to another.

Equation (1) is valid for both the gas phase and the granular phase. Total continuity will be all the volume fraction equations added. The therm ρ_{rg} is the reference density, or the volume averaged density. The right hand side of equation (1) is used where mass transfer between phases occur.

The momentum equation for the gas is like equation (2).

$$\begin{aligned}&\frac{\partial}{\partial t}\left(\alpha_g\rho_g\,\overrightarrow{u}_g\right)+\nabla\cdot\left(\alpha_g\rho_g\,\overrightarrow{u}_g\,\overrightarrow{u}_g\right) \qquad (2)\\ =\;&-\alpha_g\nabla p+\nabla\cdot\overline{\overline{\tau}}_g+\alpha_g\rho_g\,\overrightarrow{g}\\ &+\sum_{s=1}^{n}\left(K_{sg}\left(\overrightarrow{u}_s-\overrightarrow{u}_g\right)+\dot{m}_{sg}\,\overrightarrow{u}_{sg}-\dot{m}_{gs}\,\overrightarrow{u}_{gs}\right)\\ &+\left(\overrightarrow{F}_g+\overrightarrow{F}_{lift,g}+\overrightarrow{F}_{vm,g}\right)\end{aligned}$$

p is the hydrostatic pressure shared by all the phases, $\overrightarrow{g}$ is the gravitational force, $\overrightarrow{F}$ is an external body force, $\overrightarrow{F}_{lift}$ and $\overrightarrow{F}_{vm}$ is a virtual mass force. K is the interfacial momentum exchange or drag.

Equation (2) can be simplified to a simpler expression when assuming no mass transfer between the phases, no lift force and no virtual mass force. The simplified expression will be like equation (3).

$$\begin{aligned}&\frac{\partial}{\partial t}\left(\alpha_g\rho_g\,\overrightarrow{u}_g\right)+\nabla\cdot\left(\alpha_g\rho_g\,\overrightarrow{u}_g\,\overrightarrow{u}_g\right) \qquad (3)\\ =\;&-\alpha_g\nabla p+\nabla\cdot\overline{\overline{\tau}}_g+\alpha_g\rho_g\,\overrightarrow{g}\\ &+K_{sg}\left(\overrightarrow{u}_s-\overrightarrow{u}_g\right)\end{aligned}$$

The $\overline{\overline{\tau}}_g$ is the gas phase stress-strain tensor.

$$\overline{\overline{\tau}}_g=\alpha_g\mu_g\left(\nabla\overrightarrow{u}_g+\nabla\overrightarrow{u}_g^{T}\right)+\alpha_g\left(\lambda_g+\frac{2}{3}\mu_g\right)\nabla\cdot\overrightarrow{u}_g\overline{\overline{I}} \tag{4}$$

μ is the viscosity λ is the bulk viscosity $\overline{\overline{I}}$ is the unit tensor.

The assumptions for the granular phase equation (5) is the same as for the gas phase.

$$\begin{aligned}&\frac{\partial}{\partial t}\left(\alpha_s\rho_s\,\overrightarrow{u}_s\right)+\nabla\cdot\left(\alpha_s\rho_s\,\overrightarrow{u}_s\,\overrightarrow{u}_s\right) \qquad (5)\\ =\;&-\alpha_s\nabla p+\nabla\cdot\overline{\overline{\tau}}_s+\nabla p_s+\alpha_s\rho_s\,\overrightarrow{g}\\ &+K_{gs}\left(\overrightarrow{u}_g-\overrightarrow{u}_s\right)\end{aligned}$$

The momentum equation for gas and granular phase is quite similar except for the granular pressure p_s in the granular phase. The stress-strain tensor $\overline{\overline{\tau}}_s$ for the granular phase is like equation (6).

$$\overline{\overline{\tau}}_s=\alpha_s\mu_s\left(\nabla\overrightarrow{u}_s+\nabla\overrightarrow{u}_s^{T}\right)+\alpha_s\left(\lambda_s+\frac{2}{3}\mu_s\right)\nabla\cdot\overrightarrow{u}_s\overline{\overline{I}} \tag{6}$$

In the modeling of granular flow a new concept of energy is introduced, granular temperature. The normal or thermal temperature which is most common way of thinking temperature, is a measurement of the random fluctuations of the molecules in any substance. Random fluctuations will be at a micro level in the molecules. This theory is extended to the macro scale where the molecules are substituted with particles. This is called the Kinetic Theory for Granular Flow (KTGF) and is described by Lun et al. [1]. The granular temperature is a conserved scalar solved by a partial differential equation.

The conservation equation for granular temperature Θ for granular phase s, can be written as equation (7) [4].

$$\begin{aligned}&\frac{3}{2}\left[\frac{\partial}{\partial t}\left(\rho_s\alpha_s\Theta_s\right)+\nabla\cdot\left(\rho_s\alpha_s\,\overrightarrow{u}_s\Theta_s\right)\right] \qquad (7)\\ =\;&\overline{\overline{\tau}}_s:\nabla\overrightarrow{u}_s-\nabla\cdot q_s-\gamma_{\Theta_s}-3K_{sg}\Theta_s\end{aligned}$$

In words this equation (7) can be explained as equation (8).

$$\begin{aligned}&\text{Transient term + Convective term} \qquad (8)\\ =\;&\text{granular phase stress -Flux of fluctuating energy}\\ &\text{- Collisional energy dissipation}\\ &\text{+ Exchange term with phase } g\end{aligned}$$

Generation of granular temperature is due to stresses within the granular phase.

$\overline{\overline{\tau}}_s$ is the granular phase stress and can be written as equation (9).

$$\overline{\overline{\tau}}_s = [-p_s + \alpha_s \lambda_s \nabla \cdot \overrightarrow{u}_s]\overline{\overline{I}} - 2\alpha_s \mu_s \overline{S}_s \qquad (9)$$

$\overline{S}_s$ is the deformation rate and is written as equation (10).

$$\overline{S}_s = \frac{1}{2}\left[\nabla \overrightarrow{u}_s + (\nabla \overrightarrow{u}_s)^T\right] - \frac{1}{3}\nabla \cdot \overrightarrow{u}_s \overline{\overline{I}} \qquad (10)$$

The therm $\nabla \cdot q_s$ describe the diffusive flux of fluctuating or granular energy [3]. q_s can be written as equation (11).

$$q_s = k_{\Theta_s} \nabla \Theta_s \qquad (11)$$

k_{Θ_s} is the conductivity of granular temperature.

γ_{Θ_s} is the dissipation of granular temperature. Due to collisions between particles in the granular phase, the energy in the particles will dissipate. The algebraic equation for collisional energy dissipation is derived by Lun et al. [1] and showed in equation (12).

$$\gamma_{\Theta_s} = \frac{12\left(1 - e_{ss}^2\right) g_{0,ss}}{d_s\sqrt{\pi}} \rho_s \alpha_s^2 \sqrt{\Theta_s^3} \qquad (12)$$

When the restitution factor e_{ss} goes to 1, the dissipation of the granular temperature goes to zero. This means that the particles are perfectly elastic [1].

The exchange coefficient K_{sg} is the drag factor of the particles.

The restitution coefficient e_{ss} specify the the coefficient of restitution for collisions between particles.

The coefficient compensate for collisions between particles to be inelastic.

In Fluent 6.3 other properties models are included [3], but it is chosen the models most related to the kinetic theory for granular flow by [1]. The models used are

- Granular viscosity – Syamlal et al. [5]

$$\mu_s = \mu_{s,\text{col}} + \mu_{s,kin} \qquad (13)$$

$$\mu_{s,\text{col}} = \frac{4}{5}\alpha_s \rho_s g_{0,ss}\left(1 + e_{ss}\right)\sqrt{\frac{\Theta_s}{\pi}} \qquad (14)$$

$$\mu_{s,kin} = \frac{\alpha_s d_s \rho_s \sqrt{\Theta_s \pi}}{6\left(3 - e_{ss}\right)}\left[1 + \frac{2}{3}\left(1 + e_{ss}\right)\left(3e_{ss} - 1\right)\alpha_s g_{0,ss}\right] \qquad (15)$$

- Granular bulk viscosity – Lun et al. [1]

$$\lambda_s = \frac{4}{3}\alpha_s \rho_s d_s \left(1 + e_{ss}\right)\sqrt{\frac{\Theta_s}{\pi}} \qquad (16)$$

- Granular conductivity – Syamlal et al. [5]

$$k_{\Theta_s} = \frac{15 d_s \rho_s \alpha_s \sqrt{\Theta_s \pi}}{4\left(41 - 33\eta\right)}\left[1 + \frac{12}{5}\eta^2\left(4\eta - 3\right)\alpha_s g_{0,ss} + \frac{16}{15\pi}\left(41 - 33\eta\right)\eta\alpha_s g_{0,ss}\right] \qquad (17)$$

$$\eta = \frac{1}{2}\left(1 + e_{ss}\right)$$

- Radial distribution function – Lun et al. [1]

$$g_{0,ss} = \left[1 - \left(\frac{\alpha_s}{\alpha_{s,\max}}\right)^{\frac{1}{3}}\right]^{-1} \qquad (18)$$

Fluent 6.3 has an option for including models for frictional regime at high particle concentrations [3]. This will effect the viscosity and pressure in the dense part of the fluidized bed. It is assumed that this will not effect the simulations and is not included [2].

3 Description of the drag models

The drag models described here are derived in different manners. In the Master Thesis by the author [2] most of the drag models are derived in detail.

3.1 Syamlal O'Brien

The Syamlal O'Brien drag model, shown in equation (19), is derived for a single spherical particle in a fluid, and modified with a relative velocity correlation v_r. The relative velocity correlation v_r is the terminal settling velocity of a particle in a system divided by the terminal settling velocity of a single sphere [6].

$$K_{sg} = \frac{3\alpha_g \alpha_s \rho_g}{4 d_s v_r^2} C_D \left|\overrightarrow{u_s} - \overrightarrow{u_g}\right| \qquad (19)$$

In this model α_g is the volume fraction of fluid or in this case gas, α_s is the particle volume fraction, ρ_g is the fluid or gas density, d_s is the particle diameter and $|\overrightarrow{u_s} - \overrightarrow{u_g}|$ is the absolute relative interracial velocity of the particles compared to the fluid. Since this model is derived for a single spherical particle

the drag factor C_D is also a single particle model from Dalla Valle [7]. This C_D is modified with the relative velocity correlation and shown in equation (20).

$$C_D = \left[0.63 + \frac{4.8}{\sqrt{\frac{\mathrm{Re}}{v_r}}}\right]^2 \tag{20}$$

The relative velocity correlation v_r used in this model is based on a analytical model of experimental data by Richardson and Zaki [8]. This model is given by Garside and Al-Dibouni [9] and shown in equation (21).

$$\begin{aligned} v_r &= \frac{1}{2}\left[A - 0.06\,\mathrm{Re}\right] \\ &\quad + \frac{1}{2}\left[\sqrt{(0.06\,\mathrm{Re})^2 + 0.12\,\mathrm{Re}\,(2B - A) + A^2}\right] \\ A &= \alpha_g^{4.14} \\ B &= \begin{cases} 0.8\alpha_g^{1.28} & \alpha_g \leq 0.85 \\ \alpha_g^{2.65} & \alpha_g > 0.85 \end{cases} \end{aligned} \tag{21}$$

The Reynolds number used in this model is the particle Reynolds number

$$\mathrm{Re} = \frac{\rho_g d_s \left|\overrightarrow{u_s} - \overrightarrow{u_g}\right|}{\mu_g} \tag{22}$$

The main idea abut this model is the assumption that the Archimedes number is the same in a single particle and a multiparticle system. The Archimedes number relates the gravitational forces to the viscous forces [6].

3.2 Richardson Zaki

This model is similar to the Syamlal O'Brien model and the assumptions are the same. The difference is the formulation of the relative velocity correlation v_r [2]. In this model the experimental results from Richardson and Zaki are used directly. Experimental data from Richardson and Zaki provides a formula to find the v_r [8]. The formula gives v_r implicit and v_r has to be found with a algorithm [6]. The relative velocity correlation v_r is

$$v_r = \alpha_g^{n-1} \tag{23}$$

n is the Richardson Zaki parameter shown in equation (24).

$$n = \begin{cases} 4.65 & \mathrm{Re}_m < 0.2 \\ 4.4\,\mathrm{Re}_m^{-0.03} & 0.2 > \mathrm{Re}_m < 1 \\ 4.4\,\mathrm{Re}_m^{-0.1} & 1 > \mathrm{Re}_m < 500 \\ 2.4 & \mathrm{Re}_m > 500 \end{cases} \tag{24}$$

The Reynolds number used is a modified Reynolds number and is shown in equation (25).

$$\mathrm{Re}_m = \frac{\mathrm{Re}}{v_r} \tag{25}$$

Re is the particle Reynolds number described in equation (22).

The solution algorithm for the relative velocity correlation v_r is

1. Calculate particle Reynolds number.
2. Guess a initial value for the relative velocity correlation v_r e.g. 1.
3. Calculate the modified Reynolds number with equation (25).
4. Use the calculated Re_m to calculate the parameter n in equation (24).
5. Calculate right hand side of equation (23).
6. Check if the guessed v_r and the calculated v_r in step 5. match. If not use the new v_r in step 3 and calculate v_r one more time until convergence. The error accepted in this work is 10^{-5} [2].

3.3 Gidaspow

The Gidaspow drag model is a combination of the Wen and Yu drag model and the Ergun equation [10]. The Wen and Yu drag model uses a correlation from the experimental data of Richardson and Zaki. This correlation is valid when the internal forces is negligible which means that the viscous forces dominate the flow behavior. The Ergun equation is derived for a dense bed and relates the drag to the pressure drop through porous media.

The Wen and Yu drag model can be written as equation (26).

$$K_{sg} = \frac{3\rho_g \alpha_g \left(1 - \alpha_g\right)}{4 d_p} C_D \left|\overrightarrow{u_s} - \overrightarrow{u_g}\right| \alpha_g^{-2.65} \tag{26}$$

The drag factor C_D is the drag factor for a spherical particle given by [11].

$$C_D = \frac{24}{\alpha_g\,\mathrm{Re}_s}\left[1 + 0.15\left(\alpha_g\,\mathrm{Re}_s\right)^{0.687}\right] \tag{27}$$

The Ergun equation is shown in equation (28).

$$K_{sg} = 150\frac{\mu_g\left(1 - \alpha_g\right)^2}{\alpha_g\left(d_s\phi\right)^2} + 1.75\frac{\rho_g\left(\left|\overrightarrow{u_g} - \overrightarrow{u_s}\right|\right)\left(1 - \alpha_g\right)}{d_s\phi} \tag{28}$$

The Ergun equation is a combination of the Kozeny Carman equation and the Burke Plummer equation [12]. The Kozeny Carman is the first part of the Ergun equation and describe the viscous, low Reynolds number flow. The Burke Plummer equation is the second part of the Ergun equation and describe the kinetic, high Reynold number flow [13]. The constant ϕ is a shape factor for the particles. In this work it has been set to one, meaning completely spherical particles.

The combination of the two drag models (26) and (28) in the Gidaspow drag model is shown in equation (29) [10].

$$K_{sg} = \begin{cases} K_{sg}\,(\text{Wen Yu}) & \alpha_g > 0.8 \\ K_{sg}\,(\text{Ergun}) & \alpha_g \leq 0.8 \end{cases} \tag{29}$$

3.4 RUC

The RUC or Representative Unit Cell model is a drag model derived from pressure drop through porous media. It was first proposed by Du Plessis and Masliyah [14] and further developed later. The basic principles of this model is geometrical averaging of a porous media. It has the same form as the Ergun equation (28), but the two semi empirical constants (150 and 1.75) is changed with A and B. This constants are mathematically based.

$$\begin{aligned} A &= \frac{26.8\alpha_g^3}{(1-\alpha_g)^{2/3}\left(1-(1-\alpha_g)^{1/3}\right)\left(1-(1-\alpha_g)^{2/3}\right)^2} \\ B &= \frac{\alpha_g^2}{\left(1-(1-\alpha_g)^{2/3}\right)^2} \end{aligned} \tag{30}$$

This model is valid for all volume fractions of particles.

3.5 Hill Koch Ladd

The Hill Koch Ladd drag model differs somewhat from the other drag models because this is based on results from computer simulations. This is results from Lattice Boltzmann simulation. This technique is rather new because representative results from this simulations demands high computational effort [15]. The model used in this work is a modified version of the Hill Koch Ladd drag model made by the reference [15].

The modified Hill Koch Ladd model is

$$K_{sg} = \frac{3}{4}\frac{C_D\alpha_s\alpha_g\rho_g\left|\overrightarrow{u_g} - \overrightarrow{u_s}\right|}{d_p} \tag{31}$$

The drag factor C_D is modeled as

$$C_D = 12\frac{\alpha_g^2}{\mathrm{Re}_r}F \tag{32}$$

F is a dimensionless drag factor which correlates the drag to the Reynolds number and particle concentration. In this model the Reynolds number Re_r is based on the radius of the particles rather than the diameter [15].

$$\mathrm{Re}_r = \frac{\rho_g\alpha_g d_p\left|\overrightarrow{u_g} - \overrightarrow{u_s}\right|}{2\mu_g} \tag{33}$$

The model has some factors w, F_0, F_1, F_2 and F_3 shown in equation (34, 35, 36, 37, 38).

$$w = e^{(-10(0.4-\alpha_s)/\alpha_s)} \tag{34}$$

$$F_0 = \begin{cases} (1-w)\left[\frac{1+3\sqrt{\alpha_s/2}+(135/64)\alpha_s\ln(\alpha_s)+17.14\alpha_s}{1+0.681\alpha_s-8.48\alpha_s^2+8.16\alpha_s^3}\right] \\ \quad +w\left[10\frac{\alpha_s}{(1-\alpha_s)^3}\right], 0.01 < \alpha_s < 0.4 \\ 10\frac{\alpha_s}{(1-\alpha_s)^3}, \alpha_s \geq 0.4 \end{cases} \tag{35}$$

$$F_1 = \begin{cases} \frac{\sqrt{\frac{2}{\alpha_s}}}{40} & 0.01 < \alpha_s \leq 0.1 \\ 0.11 + 0.00051e^{(11.6\alpha_s)} & \alpha_g > 0.1 \end{cases} \tag{36}$$

$$F_2 = \begin{cases} (1-w)\left[\frac{1+3\sqrt{\alpha_s/2}+(135/64)\alpha_s\ln(\alpha_s)+17.89\alpha_s}{1+0.681\alpha_s-11.03\alpha_s^2+15.41\alpha_s^3}\right] \\ \quad +w\left[10\frac{\alpha_s}{(1-\alpha_s)^3}\right], \alpha_s < 0.4 \\ 10\frac{\alpha_s}{(1-\alpha_s)^3}, \alpha_s \geq 0.4 \end{cases} \tag{37}$$

$$F_3 = \begin{cases} 0.9351\alpha_s + 0.03667 & \alpha_s < 0.0953 \\ 0.0673 + 0.212\alpha_s + 0.0232/\left(1-\alpha_s\right)^5 & \alpha_s \geq 0.0953 \end{cases} \tag{38}$$

This factors are used in the drag model to model the dimensionless drag factor F which is a piecewise function of Reynolds number and particle concentration. The piecewise functions for F is shown in equation (39).

$$\begin{aligned} F &= 1 + 3/8\,\mathrm{Re}_r && \begin{cases} \alpha_s \leq 0.01 \text{ and} \\ \mathrm{Re}_r \leq \dfrac{(F_2-1)}{(3/8-F_3)} \end{cases} \\ F &= F_0 + F_1\,\mathrm{Re}_r^2 && \begin{cases} \alpha_s > 0.01 \text{ and} \\ \mathrm{Re}_r \leq \dfrac{F_3+\sqrt{F_3^2-4F_1\left(F_0-F_2\right)}}{2F_1} \end{cases} \\ F &= F_2 + F_3\,\mathrm{Re}_r && \{\text{Otherwise} \end{aligned} \tag{39}$$

4 Comparison of drag models

In the previous section the drag models was described. In the work this paper is based on a set of initial conditions used, is the same for all the drag models. Drag or interfacial momentum exchange for two phases, one gas and one particle phase, is a function of the volume fraction of gas, gas density and viscosity, slip velocity and particle diameter. For comparison, all of this are assumed to be constant except the slip velocity. The gas will move faster if the volume fraction of particles are increased. It is assumed that the slip velocity is the fluidization gas velocity divided by the gas volume fraction. The values for the properties of the flow is given in Tab. (1) [2].

The drag factor K_{sg} from the different models are given in Fig. (1) as a function of particle volume fraction.

Diameter	154 μm
Gas density	1.225 kg/m^3
Gas viscosity	1.7894x10^{-5} kg/m·s
Slip velocity	0.133/α_g m/s

Table 1: Parametrers used as the input parameters in the drag models

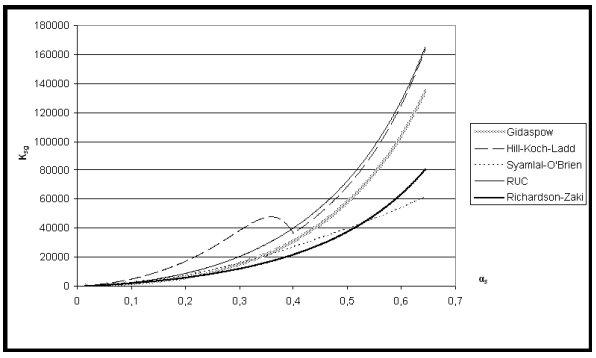

Figure 1: The different drag predicted by the different drag models [2].

The Hill Koch Ladd has the most characteristic form. At this initial values it has a local maximum at the volume fraction of particles around 0.4. This is due to the transition between low and high Reynolds flow at moderate volume fractions. It will also have a transition from low to high Reynolds flow at a lower volume fractions, but this is difficult to see at the graph. This behavior is a well known phenomena when the flow has a transition from laminar to turbulent regime.

The Gidaspow model will have a "switch" at a volume fraction of particles at 0.2 [10]. This is due to the transition between Wen Yu drag model and Ergun equation. This is not noticeable at the graph.

The Richardson Zaki drag model has four different regions, but it will change with the modified Reynolds number $\frac{\mathrm{Re}}{v_r}$. To get this clearly the initial conditions of the case has to be changed.

The Syamlal O'Brien model is based on a analytical expression based on data from Richardson Zaki and has a rather flat curve for the drag [6].

The RUC drag model is based on asymptote matching and will have a smooth curve. This model is continuous for all volume fractions [14].

The RUC and Hill Koch Ladd drag models will predict the highest drag at the volume fractions of gas which is most likely to occur in a dense fluidized bed. The problem with the Hill Koch Ladd model is that it is just valid for one particle phase [5]. In literature it is claimed that the particle size distribution will effect the results.

The Syamlal O'Brien and the Richardson Zaki models will predict the lowest drag for this initial

Diameter	154 μm
Gas density	1.225 kg/m^3
Particle density	2485 kg/m^3
Gas viscosity	1.7894x10^{-5} kg/m·s
Inlet velocity	0.133 m/s
Initial bed height	75 cm
Initial particle fraction	0.6
Operating pressure	101325 pa
Gravitational acceleration	9.81 m/s^2

Table 2: Parametrers and boundary condisions for simulation

parameters [2]. Both of this models is based on experimental data form the reference [8] from 1954, meaning the measurement equipment is from before 1954. This equipment might not be as accurate as today equipment.

4.1 Simulation results

Bubbling frequency as a function of radial position was used to compare the different models. The bubbling frequency was collected at 0.39 cm from the bottom of the bed. The computational setup is like explained in previous chapter. Experimental data from [16] is made on a bubbling fluidized bed with the dimensions [25×25×200] cm with uniform air supply in the bottom cross-section. Due to computational effort the simulation domain is simplified to 2-D. The grid used is [25×200] cm, where every cell is one by one cm. The coordinates used is Cartesian. The basic properties and boundary conditions is described in Tab. (2).

The results and experimental data from [16] is shown in Fig. (2).

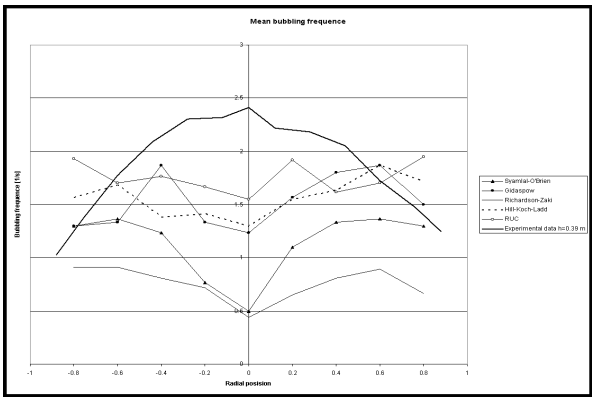

Figure 2: Results from simulations comparred to experimental results [2].

Results from the simulations the RUC, Hill Koch Ladd and Gidaspow give results closes to the experimental data from [16]. In the work this paper is based on [2] some other parameters was investi-

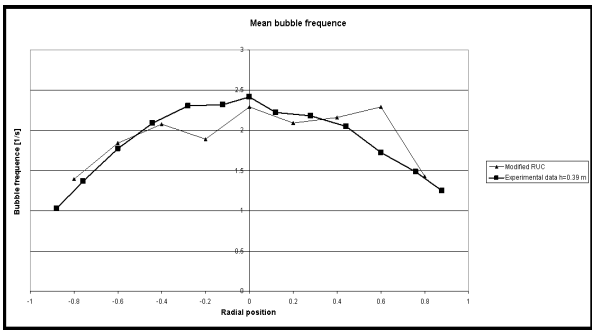

Figure 3: Modified results for the RUC model [2].

gated. This modifications was to include more particle phases regarding the size distribution particles used in the experiments have. The other thing investigated was the wall functions. By combining this results a modified result and the RUC drag model is achieved and showed in Fig.(3).

The modified results shows simulation results very close to the experimental results. The reason it is not as smooth as the experimental data might be that the experimental data is the mean bubbling frequency of 30 minutes and the simulations is for 30 seconds [2].

5 Conclusion

Five different drag models have been described, discussed and compared to each other. The drag models are Syamlal and O'Brien drag model, Gidaspow drag model, Richardson Zaki drag model, RUC drag model and Hill Koch Ladd drag model. The RUC and the Hill Koch Ladd models predicted the highest drag. Syamlal and O'Brien drag model and Gidaspow drag model are default drag models in Fluent 6.3, whereas the three other models have been implemented by the author.

Simulations with Fluent 6.3 are performed on a 2D fluidized bed with a uniform gas distribution. The results from the simulations with the different drag models are compared with respect to bubble frequencies. The computational results are also compared to experimental results. The RUC model, the Hill Koch Ladd model and the Gidaspow model give the best agreement with experimental data.

Modifications of the results achieved with the RUC model are performed. The modifications are based on the influence on bubble frequencies due to including multiple particle phases. The results are also modified to account for the effect of wall functions on bubble frequencies. The modifications are based on results from simulations with Gidaspow drag model. The modified simulation results agree very well with the experimental results.

References

[1] C. K. K. Lun, S. B. Savage, D. J. Jeffrey, and N. Chepurniy. *Kinetic Theories for Granular Flow: Inelastic Particles in Couette Flow and Slightly Inelastic Particles in a General Flow Field.* J. Fluid Mech., 140:223-256, 1984.

[2] J. Lundberg. *CFD study of a bubbling fluidized bed.* Master thesis Process Technology Høgskolen i Telemark, 2008.

[3] Fluent. *Fluent 6.3 user guide.* Fluent Inc., Lebanon, N.H, USA, 2006.

[4] J. Ding and D. Gidaspow. *A Bubbling Fluidization Model Using Kinetic Theory of Granular Flow.* AIChE J., 36(4):523-538, 1990.

[5] M. Syamlal, W. Rogers, and T. J. O'Brien. *MFIX Documentation: Volume 1, Theory Guide.* National Technical Information Service, Spring eld, VA, 1993.

[6] M. Syamlal, and T. J. O'Brien. *The Derivation of a Drag Coefficient Formula from Velocity-Voidage Correlations.* Unpublished report, April 1987.

[7] J. M. Dalla Valle. *Micromeritics.* Pitman, London, 1948.

[8] J. F. Richardson, and W. N. Zaki. *Sedimentation and Fluidization: Part I.* Trans. Inst., Chem. Eng., 32:35-53, 1954.

[9] J. Garside, and M. R. Al-Dibouni. *Velocity-Voidage Relationships for Fluidization and Sedimentation.* I & EC Process Des. Dev., 16:206-214, 1977.

[10] D. Gidaspow. *Multiphase Flow and Fluidization-Continuum and Kinetic Theory Descriptions.* Academic Press, San Diego, 1994.

[11] L. Schiller, and Z. Naumann. Ver. Deutsch. Ing., 77:318, 1935.

[12] S. Ergun. *Fluid Flow through Packed Columns.* Chem. Eng. Prog., 48(2):89-94, 1952.

[13] R. K. Niven. *Physical insight into the Ergun and Wen & Yu equation for fluid flow in packed and fluidized beds.* Chemical Eng. Science, 57:527-534, 2002.

[14] J. P. Du Plessis, and J. H. Masliyah. *Mathematical Modeling of Flow Through Consolidated Isotropic Porous Media.* Transport in Porous Media, 3:145-161, 1988.

[15] S. Benyahia, M. Syamlal, and T. J. O'Brien. *Extension of Hill Koch Ladd drag correlation over all ranges of Reynolds number and solids volume fractions.* Powder Tec., 162:166-174, 2006.

[16] B. Halvorsen. *An Experimental and Computational Study of Flow Behavior in Bubbling Fluidized Beds.* Doctoral thesis at NTNU, 2005.